INTERNATIONAL JOURNAL OF INTEGRATED ENGINEERING
ISSN: 2229-838X e-ISSN: 2600-7916

IJIE

Vol. 17 No. 4 (2025) 169-177
https://publisher.uthm.edu.my/ojs/index.php/ijie

# Influence of Parameters on Bead Geometry in Robotic GMAW Of Single-Sided Bevel T Joints with A36 Steel

**Mohd Faizal Abdul Razak[1,2]*, Irfan Rahimi Ahmad Fauzri[1], Zuraidah Salleh[1], Ahmad Hussein Abdul Hamid[1], Roslin Ramli[3]**

[1] *School of Mechanical Engineering, College of Engineering, Universiti Teknologi MARA, Shah Alam, 40450, MALAYSIA*
[2] *Department of Marine & Electrical Engineering Technology, Faculty of Marine Engineering, Universiti Kuala Lumpur, Malaysian Institute of Marine Engineering Technology, Lumut, 32200, MALAYSIA*
[3] *Department of Marine Engineering Technology, Faculty of Marine Engineering, Universiti Kuala Lumpur, Malaysian Institute of Marine Engineering Technology, Lumut, 32200, MALAYSIA*

*Corresponding Author: mfaizalar@unikl.edu.my
DOI: https://doi.org/10.30880/ijie.2025.17.04.014

**Article Info**

Received: 8 March 2025
Accepted: 29 August 2025
Available online: 19 September 2025

**Keywords**

Welding parameters, bead geometry, T-Joint, gas metal arc welding (GMAW), robotic welding

**Abstract**

This study analyses the impact of welding parameters on the quality of bevel-prepared T-joint welds. The experiments utilised a robotic welding system to ensure consistency and accuracy in the welding procedure. The welding parameters included voltage (20V-22V), current (105A and 110A), and weaving width (0.1mm - 0.3mm), while the travel speed was maintained at 2mm/s within predetermined ranges. The quality of the welds was assessed using Vickers Hardness Testing, which offers insights into the mechanical properties and microstructure of the weld zone. The findings indicate a correlation between the welding parameters and the hardness distribution across the weld bead, heat-affected zone (HAZ), and base metal. The findings indicate a significant relationship between the welding parameters and the hardness distribution throughout the weld bead, heat-affected zone (HAZ), and base metal. Variations in voltage and current have been found to impact the heat input, thereby influencing the cooling rate and, in turn, the microstructure and hardness of the weld. The travel speed significantly influenced weld bead geometry and penetration depth, subsequently affecting the overall quality of the weld. This study offers significant insights into enhancing robotic GMAW processes for T-joint welding with bevel preparation. The results can enhance weld quality and efficiency in automated welding applications across multiple industries.

## 1. Introduction

The automated arc welding process is important for quality, productivity, and cost-effectiveness because the right welding current, welding voltage, and welding speed have a big effect on how well the metal can be welded [1]. The parameters of the welding process significantly influence bead shape, such as weld penetration, bead width, horizontal leg length, vertical leg length, and throat, all of which are affected by the settings of the welding parameters. The GMAW process involves complex physical phenomena and processes resulting from melting and solidification. This may adversely affect the properties of the weld bead and base metal. The weld bead is essential for identifying the mechanical properties of the weld [2]. The geometric parameters, which involve welding penetration (WP), bead width (BW), bead height (BH), horizontal leg length (HLL), vertical leg length (VLL), and

throats are influenced by welding process parameters that include the welding current (A), welding voltage (V), travel speed (TS), weaving parameter (WP), wire extension, wire diameter, and shielding gas wire feed rate, among others. They are also referred to as welding parameters or welding variables. Consequently, it is essential to identify the appropriate welding parameters to attain optimal weld bead geometry [3]. To reduce adverse effects and achieve desired results, many studies have been conducted to monitor, predict, or control welding parameters. All these studies depend on modifying optimal welding parameters [4].

The influence of welding penetration on 6842 steels with a thickness of 2.5 mm via gas metal arc welding (GMAW) is examined. The primary factors influencing the quality of the weld joint are the GMAW welding parameters, including welding current, welding voltage, and welding travel speed. It has been found that welding parameters such as current (A), heat flux (Q), gas flow rate (G), welding speed (S), wire feed rate (F), and shielding gas can change the height (HB), width (WB), and penetration (PB) of a bead. This section addresses the relationship between welding parameter settings and welding bead geometries. The influence of welding penetration on 6842 steels with a thickness of 2.5 mm via gas metal arc welding (GMAW) is examined. The primary factors influencing the quality of the weld joint are the GMAW welding parameters, including welding current, welding voltage, and welding travel speed. Similar research and findings show that welding parameters like current (A), heat flux (Q), gas flow rate (G), welding speed (S), wire feed rate (F), and shielding gas are used to see how they affect bead height (HB), bead width (WB), and bead penetration (PB). This section addresses the relationship between welding parameter settings and welding bead geometries.

Currently, researchers are conducting various investigations regarding the T joint position. Simulation and experimentation were employed to investigate the influence of current on the morphology of an Al alloy T-joint during the double-pulsed metal inert gas (DP-MIG) welding process [5]. Another study looked at the changes in microstructure, hardness distribution, and grain growth in weld joints [7]. This one used both experimental tests and numerical simulations to look at the residual stress and distortion caused by welding in T-joint welds [6]. Extensive research has been conducted on the T joint position; however, there are no documented instances of single bevel preparation with weaving application.

Weaving techniques have been developed to prevent challenging welds and potential defects, thereby enhancing the proficiency of welders. The welder employs weaving techniques to cover a broader area and execute shelter welds over stringer beads (multi-pass welding). In other words, welders use this technique when applying multiple layers of welds. Welders frequently use these weaving techniques when multiple welds occur on the same seam [8]. Numerous welding weaving techniques exist, including sine function weaving, circular weaving, and zigzag weaving; however, the choice of technique depends on the material type, welding process, welding position, and weld joint. Various methods have been used in performing a weaving technique.

Semi-automatically moves the torch back and forth along the weld joint. A variety of mechanisation levels are commercially available. These machines mechanically oscillate the torch back and forth while concurrently advancing the electrode along the weld joint. Numerous joining and surface applications commonly employ a weaving technique [9,10]. The application determines the weaving technique employed and the weaving effect produced. The most common technique for weaving is the open root butt joint, whereby the electrode is passed through the open joint and secured on both sides to ensure adequate penetration into the two components being joined, while preventing burn-through of the joint [11]. The Gas Metal Arc V-groove welding processes, both with and without root gaps, have been examined through three-dimensional numerical simulations utilizing the volume of fluid method for flat welding positions [12]. Similar investigations were conducted on V groove joints without backing plates, where the authors employed Metal Active Gas (MAG) welding with the switch-back welding technique [13]. The weave technique directs the arc's heat away from the weld's centre to produce a flat bead shape. In overlay and hard facing applications, a weave is employed to segregate weld metal from the base metal across a large surface area with minimal interaction. In every one of these situations, a weaving technique was employed to redirect the arc's heat from the centre of the weld to its peripheries. The success of a weaving technique is limited by the extent to which heat can be controlled through movement. However, there exists a requirement for an enhanced welding system and methodology that distinctly differentiates heat input between the edges of a weaving technique and the centre.

The critical requirement is the selection of good welding parameters to produce the desired bead geometry. A change in welding parameters can result in a significant change in bead geometry; the output profile may have poor penetration, the wrong size, or internal defects. This work will investigate the welding parameters and weld deposition geometry in the 2F position. To the knowledge of the author, no literature review has been reported on the result when the weaving techniques are applied to the T-joint configuration with the single bevel preparation.

This research focused on welding parameters that are shown in Table 1 and welding deposition geometry for T-joint by FANUC Robotics series with the application of the Gas Metal Arc Welding (GMAW) process function. The consumable is a 1.2mm diameter ER70S-6 filler wire, and the shielding gas is 100% carbon dioxide. The base material is a low-carbon steel plate (A36). The T-Joint is positioned in 2F welding positions. The output is a

Int. Journal of Integrated Engineering Vol. 17 No. 4 (2025) p. 169-177

welding bead geometry for the respective welding parameter. The quality of welding will be evaluated by visual inspection, with the American Welding Society (AWS D1.1) codes as a reference.

## 2. Methodology

A robotic welding machine was employed to perform GMAW welding, and the power source used in this study was a Kemmpi, as shown in Fig. 1. This machine can be programmed with Welding Current (A), Welding Voltage (V), Travel Speed (TS), and Weaving Parameter (WP). All the welding data were recorded with direct reference to the respective sample number.

**(a)** **(b)**

**Fig. 1** *Robotic welding machine (a) Robotic GMAW welding arm; (b) Power source, Kemmpi*

**Table 1** *Welding specification*

| No | Variables | Descriptions |
|---|---|---|
| 1 | Welding parameters | Currents (105 – 110 A)<br>Voltages (20 – 22 V)<br>Travel speeds (2 mm/s)<br>Weaving Parameters (0.1-0.3 mm)<br>Wire extensions (12.5 mm) |
| 2 | Consumable types | GMAW wire (E70T-1)<br>Diameter: 1.2mm<br>SFA No: A5.20<br>Developer: ESAB |
| 3 | Polarity | Direct Current Reverse Polarity (DCEP) |

The welding parameters were categorised into 18 sets of welded coupons, each including different welding currents, welding voltages, and weaving parameters for every welding sample. All welding parameters on each weld coupon were maintained constant, with only one parameter being varied. Every coupon was assigned a reference number. During the welding process, the actual welding parameters were monitored and updated to ensure that the record precisely represented the actual welding conditions. An automated system controlled the speed of the welding, making it reliable and accurate. The voltage changed very little, and only the current deviated significantly from the set parameters, so the welding current had to be adjusted. A low-carbon steel base plate was identified, and its chemical composition was determined using an Arc Spectrometry machine. Table 2 displays the results of the composition analysis for the chosen base material. The outcome verified that it is low-carbon steel with excellent weldability.

**Table 2** *Chemical composition (%)*

| C | Si | Mn | P | S | Cr | Mo | Ni |
|---|---|---|---|---|---|---|---|
| 0.164 | 0.165 | 0.461 | 0.0125 | 0.0683 | 0.0879 | 0.0179 | 0.0874 |

The test specimens were welded by a robotic welder in the 2F position (horizontal). The plate was low carbon steel, measuring 5 mm in thickness, 150 mm in length, and 50 mm in width. A 25 mm piece from each coupon was macro-etched to check the quality of the weld deposit and bead penetration and to find out what the whole bead shape was. BS EN 970 requires that during a visual inspection, the minimum illumination must be 500 lux or equivalent to standard shop or office lighting.

The procedure for observing the microstructure in the experiment involved several sequential steps. Initially, specimens were prepared by reducing them to smaller dimensions. The preparation continued with a grinding phase using sandpapers of varying grits (180, 240, 320, 400, 600, and 1200), followed by polishing with micron-sized particles (5, 3, and 1 micron) using the Buehler Metaserv 2000 rotary grinder machine. Before conducting the test, we grind the sample to ensure a flat surface and polish it to achieve a reflective, mirror-like finish. Further treatment involved etching the specimens using a 15% nital etchant solution, enhancing visibility for microstructure analysis. Finally, the microstructures were observed under an optical microscope magnification of 50x, enabling an in-depth examination for comprehensive analysis. Researchers used Vickers Hardness test to determine the hardness of specimens.

## 3. Results and Analysis

### 3.1 Microstructure

The macrostructural analysis involves comprehensive scrutiny and assessment of the overall structure and attributes of a material or component at a macroscopic scale. This analytical process delves into the observable features, encompassing the size, shape, and distribution of structural elements like weld beads geometry [14].

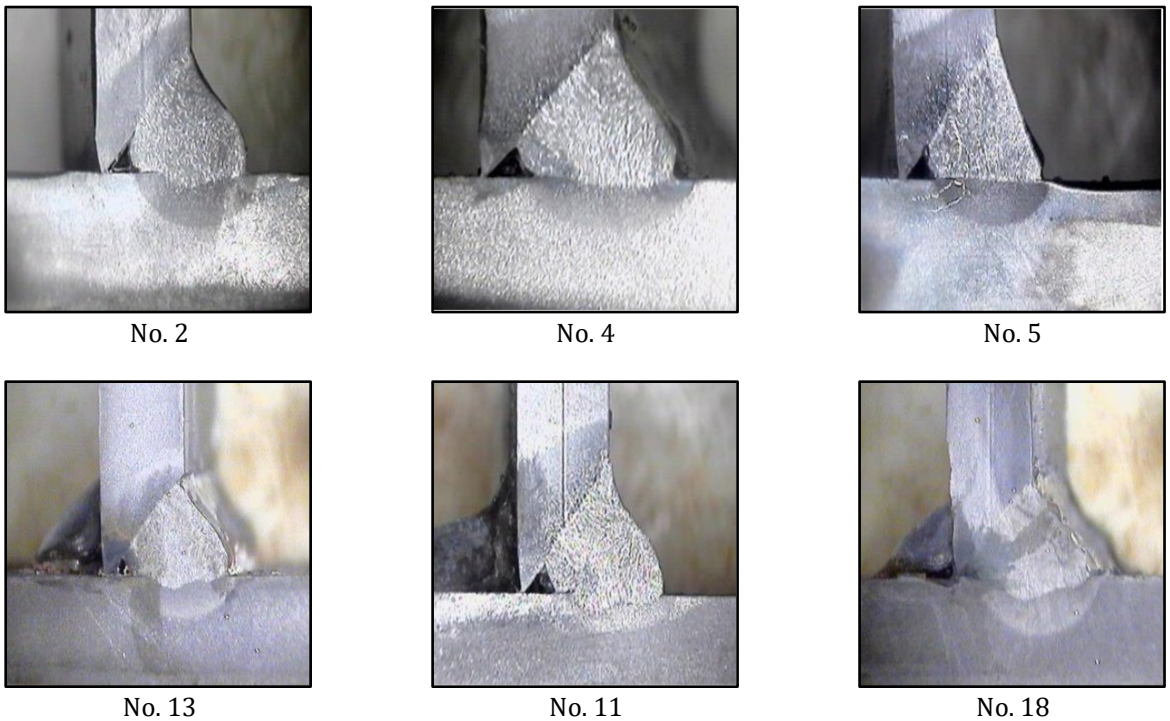


**Fig. 2** *Selected specimen with incomplete root penetration*

Based on Fig. 2, the macrostructure of the selected specimens above indicates that most of the welding does not fill adequately the desired space of the specimens, which is between the bevel plate and the normal plate. This defect occurs when the weld metal fails to fuse with the root of the joint. The welding parameters (current, voltage, travel speed) are not optimized, there may be insufficient heat to fully melt the root of the joint. This is particularly

Int. Journal of Integrated Engineering Vol. 17 No. 4 (2025) p. 169-177

problematic due to the thickness of material at the intersection [15]. A root gap that is too small also can prevent proper penetration for T joint configuration [15]. In robotic welding, the programmed path and angle of the welding torch can significantly affect root penetration. If not optimized, it may lead to incomplete fusion at the root.

**Table 3** *Weld bead geometries value*

| No | HLL (mm) | VLL (mm) | AT (mm) | TT (mm) | ET (mm) |
|---|---|---|---|---|---|
| 1 | 3.77 | 6.17 | 6.51 | 5.49 | 6.00 |
| 2 | 3.53 | 6.53 | 6.34 | 5.49 | 6.00 |
| 3 | 3.27 | 7.64 | 6.86 | 6.34 | 6.17 |
| 4 | 2.91 | 7.71 | 6.51 | 5.66 | 6.69 |
| 5 | 2.83 | 6.50 | 6.67 | 6.33 | 5.83 |
| 6 | 3.19 | 6.75 | 6.75 | 6.34 | 6.94 |
| 7 | 3.38 | 5.23 | 6.62 | 6.28 | 6.00 |
| 8 | 3.57 | 6.32 | 6.81 | 6.00 | 6.16 |
| 9 | 3.55 | 6.82 | 6.82 | 6.41 | 6.14 |
| 10 | 3.27 | 5.24 | 6.55 | 6.11 | 5.89 |
| 11 | 3.43 | 6.51 | 6.69 | 6.00 | 6.34 |
| 12 | 2.76 | 7.56 | 6.48 | 5.28 | 7.08 |
| 13 | 3.43 | 7.20 | 6.17 | 5.31 | 6.69 |
| 14 | 4.16 | 6.49 | 6.49 | 6.12 | 6.00 |
| 15 | 4.42 | 7.11 | 7.11 | 6.79 | 7.26 |
| 16 | 4.82 | 8.82 | 7.64 | 6.24 | 7.17 |
| 17 | 4.75 | 4.88 | 7.25 | 7.13 | 6.13 |
| 18 | 4.59 | 6.71 | 7.41 | 7.24 | 6.88 |

Analysing the data from the 18 specimens, it is evident that the values for Actual Throat (AT) and Theoretical Throat (TT) exhibit variations based on the specific welding and weaving parameters employed as shown in Table 3. Notably, 18 demonstrates the smallest discrepancy between the two throats, with a mere 0.32mm difference. Conversely, specimen no. 12 presents the most significant disparity, recording a substantial 1.2 mm difference. These findings suggest a discernible correlation between the applied voltage and the discrepancy between actual and theoretical throat values. Specifically, it appears that a higher voltage utilized in conjunction with a 110A current tends to yield a minimized difference between the actual and theoretical throat measurements [16]. This insight underscores the importance of voltage parameters in achieving a closer alignment between the intended and observed outcomes in welding and weaving processes.

The dataset has a wide range of Horizontal Leg Lengths (HLL). Specimen no. 12 has the shortest HLL, measuring 2.76 mm, which means that shorter horizontal extensions could change the structure, while specimen no. 16 has the longest HLL, measuring 4.82 mm, which means that longer horizontal extensions could change the strength of the joint. The overall range, along with a mean HLL of about 3.61 mm, shows how different the welding results can be. Thus, it shows that high voltage and current affect the Horizontal Leg Length (HLL) [24]. Additionally, the Vertical Leg Lengths (VLL) across specimens display a notable range, from the minimum of 4.88mm in specimen no 17 indicating shorter vertical leg lengths possibly due to less penetration or different techniques, to the maximum of 8.82 mm in specimen no. 16 suggesting deeper penetration or variations in welding parameters, highlighting diversity in the height dimensions of the weld beads. Effective Throat (ET) is the shortest distance from the root to the face of the weld. Based on the data above, the value for Effective Throat (ET) among the 18 specimens that were subjected to calculation, a subset of 4 specimens specifically, specimen no. 1, specimen no. 2, specimen no. 17 and specimen no. 14 exhibits identical values corresponding to the plate thickness, measured at 6.00 mm. This uniformity in results suggests a consistent welding outcome for these specimens which results in stronger welding as the bigger the throat, the larger the effective area. The Effective Throat (ET) value for specimen no. 5 was the lowest, at 5.83 mm. This suggests that the specimen may not have a strong weld

compared to the other specimens, but a higher Effective Throat (ET) value does not always mean that the welding is stronger. Upon meticulous examination of the data, it becomes evident that the relationship between Horizontal Leg Length (HLL) and Effective Throat (ET) is not consistently correlated, as exemplified by specimen no. 1, specimen no. 2, specimen no 7, and specimen no. 14. Despite displaying distinct values for Horizontal Leg Length (HLL) of 3.77 mm, 3.53 mm, 3.38 mm, and 4.16 mm, these specimens share an identical Effective Throat (ET) value of 6.00 mm. The observation challenges the conventional assumption that a higher Horizontal Leg Length (HLL) necessarily corresponds to a greater Effective Throat (ET). The existence of specimens with varying HLL values but the same ET suggests a nuanced interplay of welding parameters and intricate factors influencing the weld geometry. This highlights the complexity of the welding process, where achieving a specific Horizontal Leg Length does not guarantee a proportional increase in the Effective Throat.

## 3.2 Vickers Hardness Test

The Vickers hardness test is a commonly used technique for assessing the hardness of materials by using a diamond pyramid-shaped indenter to create an impression on the surface. The hardness number comes from dividing the load by the area of the impression. This gives a precise picture of how resistant a material is to deform plastically [17]. This method, frequently used for hardness measurement, provides essential information about the mechanical properties and durability of materials in various applications [18]. Welding parameters significantly influence Vickers hardness, with increased values in the heat-affected zone and weld attributed to rapid cooling, leading to finer grain size development. Furthermore, the hardness of the weld metal may be subject to influences from factors like precipitation hardening effects, residual stresses, and the microstructural refinement resulting from the accelerated cooling of the weld metal [19]. The complex interplay between welding parameters and material hardness is highlighted, with the table presenting Vickers Hardness Test values for 18 specimens as shown in Table 4. The test involved five indentations forming a straight line across base metal, Heat-Affected Zone (HAZ), and welded joints.

**Table 4** *Vickers hardness test*

| No | Base metal horizontal plate (mm) | HAZ on horizontal plate (mm) | Welded joints (mm) | HAZ on Vertical plate (mm) | Base metal vertical plate) (mm) |
|---|---|---|---|---|---|
| 1 | 160.3 | 153.1 | 180.8 | 161.5 | 147.5 |
| 2 | 154.3 | 185.0 | 213.9 | 257.9 | 260.6 |
| 3 | 158.3 | 157.6 | 177.2 | 203.6 | 160.4 |
| 4 | 143.5 | 253.0 | 227.6 | 223.1 | 160.9 |
| 5 | 162.4 | 173.6 | 200.8 | 203.8 | 161.9 |
| 6 | 181.4 | 170.9 | 178.8 | 189.4 | 172.2 |
| 7 | 130.8 | 160.9 | 170.4 | 149.7 | 141.3 |
| 8 | 154.7 | 199.6 | 194.9 | 158.0 | 183.8 |
| 9 | 152.2 | 192.4 | 181.2 | 164.1 | 163.9 |
| 10 | 160.9 | 182.3 | 195.1 | 219.0 | 199.4 |
| 11 | 192.6 | 187.3 | 236.3 | 179.3 | 174.6 |
| 12 | 165.3 | 158.4 | 155.3 | 167.9 | 155.6 |
| 13 | 195.3 | 176.2 | 193.1 | 182.9 | 162.9 |
| 14 | 153.4 | 178.1 | 190.1 | 139.2 | 135.5 |
| 15 | 148.9 | 162.9 | 213.3 | 188.4 | 164.0 |
| 16 | 175.1 | 181.6 | 244.8 | 196.2 | 210.5 |
| 17 | 159.8 | 196.1 | 203.1 | 165.6 | 161.8 |
| 18 | 202.4 | 197.8 | 205.7 | 179.0 | 202.9 |

The Vickers Hardness Test results, as depicted in the provided table, offer valuable insights into the material's properties at various locations across the examined specimens. The measurements, shown by the Vickers Hardness values, show that the hardness is not evenly distributed across the different areas. These areas include the base metal, the heat-affected zones (HAZ), and the welded joints. Specimens exhibit distinct hardness characteristics, with notable variations observed within each specimen.

In analysing the table, it becomes apparent that specimens no. 1, no. 11, and no. 16 showcase higher Vickers hardness values, indicating greater resistance to deformation and wear in these regions. These specimens stand out as potential candidates for applications demanding enhanced mechanical strength and durability, such as tools, machine components, or surfaces requiring resistance to wear [20]. Conversely, specimen no. 14 and specimen no. 15 demonstrate relatively lower Vickers hardness values, suggesting a softer material characteristic in these zones. It's important to know how these specimens' hardness varies for uses that require flexibility or malleability. Upon observation, a discernible trend emerges, indicating that the hardness value of the welded part is the highest compared to both the heat-affected zone and the base metal [21]. However, it is noteworthy that the heat-affected zone should exhibit a higher hardness when compared to the base metal, as exemplified in specimen no. 15. The variations in hardness values across different locations within each specimen also merit attention. For instance, specimen no. 2 displays a substantial difference in hardness between the base metal horizontal plate and the welded joints, indicating potential variations in the metallurgical properties induced by the welding process.

In summary, the Vickers Hardness Test results reveal varied hardness across specimens, guiding material selection and process optimisation for welded components to meet application-specific requirements [22]. Distinct attributes in specimens no. 4, no. 11, and no. 16 underscore the importance of customised welding parameters for desired material characteristics, showcasing practical implications for industries seeking specific hardness profiles. Strategically optimising weld parameters for higher Vickers hardness values can enhance the excellence and efficacy of welded materials [5].

## 4. Conclusion

The objective of this study. was to discern optimal welding parameters that yield high-quality weldments and to establish correlations between welding parameters and bead geometry in gas metal arc welding (GMAW) with the application of the weaving method [23]. Following a comprehensive experimental and research phase, the findings unequivocally indicate that employing a lower current and voltage results in the most favourable welding outcomes. Furthermore, the introduction of the weaving method significantly enhances the weldment, surpassing the quality achieved without this method. Remarkably, the weld geometries table highlights the distinct attributes of specimen no. 3, specimen no. 6, and specimen no. 7, showcasing an overall exceptional quality and strength in welds. This underscores the significance of carefully selecting and optimizing welding parameters to achieve superior results, particularly when employing the weaving method [24]. The investigation extends to the examination of the Heat-Affected Zone (HAZ), revealing that lower current and voltage not only contribute to favorable weld outcomes but also yield a clearer HAZ. This clarity in the HAZ becomes pivotal for subsequent testing and assessments, providing valuable insights into the thermal effects of the welding process. A critical aspect explored in this study is the Vickers Hardness Test, where the analysis concludes that a higher Hardness Value (HV) is advantageous, indicative of greater resistance to deformation and wear [21]. This aligns with broader materials engineering principles; wherein elevated hardness values correlate with heightened mechanical strength and durability. The implication is that materials exhibiting such characteristics are well-suited for applications where hardness is a critical factor, such as in tools, machine components, and surfaces requiring resistance to wear. In conclusion, getting higher Vickers hardness values by carefully calibrating welding parameters and processes becomes a must from a business point of view. This not only ensures the quality and performance of welded materials but also positions the welded components favourably for deployment in demanding applications. The nuanced insights gleaned from this study provide a foundation for informed decision-making in welding applications, emphasising the importance of parameter optimisation and weaving techniques for achieving superior weld quality, structural integrity, and hardness characteristics.

## Acknowledgement

The authors would like to thank Universiti Teknologi Mara and Universiti Kuala Lumpur for their facilities support.

## Conflict of Interest

The authors declare that there is no conflict of interest regarding the publication of the paper.

## Author Contribution

*The authors confirm contribution to the paper as follows:* ***study conception and design:*** *Mohd Faizal Abdul Razak, Zuraidah Salleh;* ***data collection:*** *Irfan Rahimi Ahmad Fauzri;* ***analysis and interpretation of results:*** *Irfan Rahimi Ahmad Fauzri, Zuraidah Salleh;* ***draft manuscript preparation:*** *Mohd Faizal bin Abdul Razak, Zuraidah Salleh, Roslin Ramli. All authors reviewed the results and approved the final version of the manuscript.*

## References

[1] Xiong, J., Zhang, G., Hu, J., & Wu, L. (2014). Bead geometry prediction for robotic GMAW-based rapid manufacturing through a neural network and a second-order regression analysis. *Journal of Intelligent Manufacturing*, *25*, 157-163, https://doi.org/10.1007/s10845-012-0682-1

[2] Martínez, R. T., Bestard, G. A., Silva, A. M. A., & Alfaro, S. C. A. (2021). Analysis of GMAW process with deep learning and machine learning techniques. *Journal of Manufacturing Processes*, *62*, 695-703, https://doi.org/10.1016/j.jmapro.2020.12.052

[3] Rao, P. S., Gupta, O. P., Murty, S. S. N., & Rao, A. K. (2009). Effect of process parameters and mathematical model for the prediction of bead geometry in pulsed GMA welding. *The International Journal of Advanced Manufacturing Technology*, *45*, 496-505, https://doi.org/10.1007/s00170-009-1991-1

[4] Martínez, R. T., Bestard, G. A., Silva, A. M. A., & Alfaro, S. C. A. (2021). Analysis of GMAW process with deep learning and machine learning techniques. *Journal of Manufacturing Processes*, *62*, 695-703, https://doi.org/10.1016/j.jmapro.2020.12.052

[5] Wordofa, T. N., & Ramulu, P. J. (2023). Gas metal arc welding input parameters impacts on weld quality characteristics of steel materials a comprehensive exploration. *Technology*, *3*(23), 366-379, https://doi.org/10.21062/mft.2023.046

[6] Azad, N., Iranmanesh, M., & Rahmati Darvazi, A. (2020). A study on the effect of welding sequence on welding distortion in ship deck structure. *Ships and Offshore Structures*, *15*(4), 355-367, https://doi.org/10.1080/17445302.2019.1619898

[7] Winarto, W., Oktadinata, H., & Siradj, E. S. (2018, June). Microstructure and hardness properties of butt and fillet GMAW welded joints on HY80 high strength steel plate. In *AIP Conference Proceedings* (Vol. 1977, No. 1). AIP Publishing. https://doi.org/10.1063/1.5046656

[8] Jin, C., & Rhee, S. (2021). Real-time weld gap monitoring and quality control algorithm during weaving flux-cored arc welding using deep learning. *Metals*, *11*(7), 113, https://doi.org/10.3390/met11071135

[9] Jiao, C., & Li, H. (2021, December). A Trajectory Planning Method for Industrial Robot Weaving Welding Based on Piecewise Function. In *2021 IEEE International Conference on Robotics and Biomimetics (ROBIO)* (pp. 1605-1610). IEEE. https://doi.org/10.1109/ROBIO54168.2021.9739278

[10] Kang, C., Liu, Z., Chen, S., & Jiang, X. (2019). Circular trajectory weaving welding control algorithm based on space transformation principle. *Journal of Manufacturing Processes*, *46*, 328-336, https://doi.org/10.1016/j.jmapro.2019.08.027

[11] Urbański, T., Graczyk, T., Taraska, M., & Iwańkowicz, R. (2018). Assessment of technological usefulness of panel production line in shipbuilding process. *Polish Maritime Research*, *25,* 134-144, https://doi.org/10.2478/pomr-2018-0034

[12] Cho, D. W., Na, S. J., Cho, M. H., & Lee, J. S. (2013). A study on V-groove GMAW for various welding positions. *Journal of Materials Processing Technology*, *213*(9), 1640-1652, https://doi.org/10.1016/j.jmatprotec.2013.02.015

[13] Yamane, S., Uji, K., Nakajima, T., & Yamamoto, H. (2015). Application of switch back welding to V groove MAG welding. *Welding International*, *29*(2), 103-109, https://doi.org/10.1080/09507116.2012.753253

[14] Chaudhari, R., Parmar, H., Vora, J., & Patel, V. K. (2022). Parametric study and investigations of bead geometries of GMAW-based wire–arc additive manufacturing of 316L stainless steels. *Metals*, *12*(7), 1232, https://doi.org/10.3390/met12071232

[15] Pradhan, R., Joshi, A. P., Sunny, M. R., & Sarkar, A. (2022). Performance of predictive models to determine weld bead shape parameters for shielded gas metal arc welded T-joints. *Marine Structures*, *86*, 103290, https://doi.org/10.1016/j.marstruc.2022.103290

[16] Oh, W. J., Lee, C. M., & Kim, D. H. (2022). Prediction of deposition bead geometry in wire arc additive manufacturing using machine learning. *Journal of Materials Research and Technology*, *20*, 4283-4296.

[17] Ramli, R., Mohd Hashim, M. H., Alisibramulisi, A., Mohamed Noor, S., & Abdul Razak, M. F. (2022). Tensile strength testing of+ 45 isotropic FRP laminate on different universal testing machines. In *Design in Maritime Engineering: Contributions from the ICMAT 2021* (pp. 69-81). Cham: Springer International Publishing. https://doi.org/10.1007/978-3-030-89988-2_6

[18] Meseguer-Valdenebro, J. L., Martínez-Conesa, E., & Portoles, A. (2022). Influence of welding parameters on grain size, HAZ and degree of dilution of 6063-T5 alloy: optimization through the Taguchi method of the GMAW process. *The International Journal of Advanced Manufacturing Technology*, *120*(9), 6515-6529, https://doi.og/10.1007/s00170-022-09094-3

[19] Hussein, N. I. S., Ket, G. C., Rahim, T. A., Ayof, M. N., Abidin, M. Z. Z., & Srithorn, J. (2023). Process and Heat Resources for Wire Arc Additive Manufacturing of Aluminium Alloy ER4043: A Review. *Journal of Mechanical Engineering (1823-5514)*, *20*(1), https://doi.org/10.24191/jmeche.v20i1.21077

[20] Tenong, F. F. S. B., Hikmawati, D., & Setiawati, E. M. (2021, February). Characterization of vickers hardness and corrosion rate of stainless steel-316L coated with hydroxyapatite-polyvinyl alcohol. In *Journal of Physics: Conference Series* (Vol. 1816, No. 1, p. 012012). IOP Publishing. https://doi.org/10.1088/1742-6596/1816/1/012012

[21] Dovale-Farelo, V., Tavadze, P., Lang, L., Bautista-Hernandez, A., & Romero, A. H. (2022). Vickers hardness prediction from machine learning methods. *Scientific Reports*, *12*(1), 22475,

https://doi.org/10.1038/s41598-022-26729-3

[22] Chicot, D., Roudet, F., Soom, A., & Lesage, J. (2007). Interpretation of instrumented hardness measurements on stainless steel with different surface preparations. *Surface Engineering*, *23*(1), 32-39, https://doi.org/10.1179/174329407X161573

[23] Khrais, S., Al Hmoud, H., Abdel Al, A., & Darabseh, T. (2023). Impact of gas metal arc welding parameters on bead geometry and material distortion of AISI 316L. *Journal of Manufacturing and Materials Processing*, *7*(4), 123, https://doi.org/10.3390/jmmp7040123

[24] Xydea, E., Panagiotopoulou, V. C., & Stavropoulos, P. (2024). A strategy framework for identifying carbon intensive elements in welding processes. *Procedia CIRP*, *121*, 103-108, https://doi.org/10.1016/j.procir.2023.09.236